

Complex Molecules in the L1157 Molecular Outflow

Héctor G. Arce

Department of Astronomy, Yale University, P.O. Box 208101, New Haven, CT 06520-8101

hector.arce@yale.edu

Joaquín Santiago-García

Observatorio Astronómico Nacional, Alfonso XII 3, E-28014 Madrid, Spain

j.santiago@oan.es

Jes K. Jørgensen

Argelander-Institut für Astronomie, University of Bonn, Auf dem Hügel 71, 53121 Bonn, Germany

jes@astro.uni-bonn.de

Mario Tafalla

Observatorio Astronómico Nacional, Alfonso XII 3, E-28014 Madrid, Spain

m.tafalla@oan.es

and

Rafael Bachiller

Observatorio Astronómico Nacional, Alfonso XII 3, E-28014 Madrid, Spain

r.bachiller@oan.es

ABSTRACT

We report the detection of complex organic molecules in the young proto-stellar outflow L1157. We identify lines from HCOOCH_3 , CH_3CN , HCOOH and $\text{C}_2\text{H}_5\text{OH}$ at the position of the B1 shock in the blueshifted lobe, making it the first time that complex species have been detected towards a molecular outflow powered by a young low-mass protostar. The time scales associated with the warm outflow gas ($< 2 \times 10^3$ yr) are too short for the complex molecules to have

formed in the gas phase after the shock-induced sputtering of the grain mantles. It is more likely that the complex species formed in the surface of grains and were then ejected from the grain mantles by the shock. The formation of complex molecules in the grains of low-mass star forming regions must be relatively efficient, and our results show the importance of considering the impact of outflows when studying complex molecules around protostars. The relative abundance with respect to methanol of most of the detected complex molecules is similar to that of hot cores and molecular clouds in the galactic center region, which suggests that the mantle composition of the dust in the L1157 dark cloud is similar to dust in those regions.

Subject headings: ISM: molecules — stars: formation — ISM: jets and outflows — ISM: individual (L1157) — astrochemistry

1. Introduction

Shocks from protostellar outflows heat and compress the surrounding medium thereby triggering different processes (e.g., grain disruption, ice gain mantle sublimation, etc.) that can release molecules trapped in the grains into the gas phase. In this way, outflows contribute to the chemical enrichment of the gaseous environment surrounding young stars. This is clearly demonstrated by multi-molecular line observations reflecting enhanced molecular abundances either in shocks associated with the outflows or in the outflow cavity walls in the protostellar envelopes (e.g., Garay et al. 1998; Bachiller et al. 2001; Arce & Sargent 2006; Jørgensen et al. 2007). In most cases these molecules have similar velocity and structure as the CO lines that trace the outflows, and it is clear that the outflow is responsible for their overabundance.

The limited outflow chemistry studies show shock-triggered overabundance of parent (or “first generation”) species —molecules that are released directly into the gas phase from the icy dust mantles, like H_2CO and CH_3OH — as well as other simple molecules presumably formed in the warm gas (e.g., SO , HCO^+). Chemical models indicate that larger organic molecules (made of 7 atoms or more) can form on grain surfaces (e.g., Garrod & Herbst 2006) and should be present in the gas phase along with the other simpler molecules observed near outflow shocks —as suggested by Chandler et al. (2005) and Remijan & Hollis (2006). Yet, up to date, conclusive evidence for shock-triggered overabundances in molecular outflows from low-mass stars ($M < 2M_\odot$) exists only for species with six atoms or less. Here we report the first detection of HCOOH , CH_3CN , HCOOCH_3 , $\text{C}_2\text{H}_5\text{OH}$ in the the L1157 molecular outflow.

The L1157 dark cloud (at a distance of about 440 pc) harbors an embedded low-mass stellar object, L1157-mm (IRAS 20386+6751), that powers a young molecular outflow (Umemoto et al. 1992). The powerful L1157 outflow is comprised of several shocks seen as bright knots in near and mid infrared images (Davis & Eisloffel 1995; Cabrit et al. 1998; Looney et al. 2007). Millimeter observations of many molecular emission lines show that L1157 is a chemically rich outflow exhibiting an overabundance of SiO, CH₃OH, H₂CO, CN, HCN, SO, and a number of other species by a factor of a few tens to more than 10⁵, depending on the molecule (Bachiller & Pérez Gutiérrez 1997, hereafter BP97). In the blue (southern) lobe, the emission from these species is brightest towards two to three clumps (Bachiller et al. 2001), and high-resolution interferometer observations reveal the clumps are associated with shell-like structures created by two jet-driven bow shocks (Zhang et al. 1995; Gueth et al. 1996). These results indicate that the observed chemical enhancements are induced by the outflow shocks.

2. Observations and Results

Observations of the lines shown in Table 1 were obtained using the IRAM 30 m telescope in Pico Veleta, Spain, in June 2007. Our observations concentrated in the brightest CO clump in the blue lobe of the L1157 outflow (i.e., the B1 clump), located at an offset of $\Delta\alpha = 22.5''$, $\Delta\delta = -64.5''$ from the L1157-mm protostar at $\alpha(\text{J2000}) = 20^{\text{h}}39^{\text{m}}06^{\text{s}}.2$, $\delta(\text{J2000}) = 68^{\circ}02'16''$ (Bachiller et al. 2001). The B1 clump is far enough from the source and the telescope beam is sufficiently small (see below) that any molecular line emission associated with the gas immediately surrounding L1157-mm (i.e., within 10⁴ AU) does not contaminate our observations. Two different spectral configurations were used in order to include as many line transitions as possible of HCOOH, C₂H₅CN, CH₃CN, and HCOOCH₃ (A and E) —complex molecules that have been detected in the immediate surroundings of deeply embedded low-mass protostars (Cazaux et al. 2003; Bottinelli et al. 2007). Both spectral configurations included four receivers, each simultaneously connected to a 256 channel filter bank with a spectral resolution of 1 MHz and a unit of an autocorrelator, that provided simultaneous observations at four different frequencies ranging from 90.1 to 257.6 GHz. The autocorrelator was set to provide spectral resolutions of 40 and 320 kHz and bandwidths between 40 and 320 MHz. All observations were obtained in wobbler switching mode with a 90'' throw —large enough to avoid any possible “contaminating” emission from the rest of the blueshifted lobe or the immediate surroundings of L1157-mm. Verification of the telescope pointing approximately every two hours, indicated that the pointing accuracy was between 2 and 4''. A total integration time of four to ten hours, and average system temperatures between 120 K and 830 K, depending on the frequency, resulted in spectra with rms of 0.002

to 0.01 K. The telescope beamwidth (FWHM) at 90.2, 98.6, 135.7, 226.7, and 257.5 GHz is 27'', 25'', 18'', 11'', and 10'', respectively. Spectral data presented here are in units of main beam brightness temperature, T_{mb} (see Rohlfs & Wilson 2000).

We detect, at a 3σ level or higher, five HCOOCH_3 -A transitions, four HCOOCH_3 -E transitions, three CH_3CN transitions, two HCOOH transitions and one $\text{C}_2\text{H}_5\text{OH}$ transition (see Table 1). These were identified using the CDMS and JPL catalogs (Müller et al. 2001; Pickett et al. 1998). We are confident that the emission arises from the L1157 outflow's blue lobe as all lines are blueshifted by 1.5 to 4.0 km s^{-1} with respect to the L1157 cloud central velocity ($V_{LSR} = 2.7 \text{ km s}^{-1}$) and have a velocity width between 2 and 7 km s^{-1} as expected from the velocity distribution of other species associated with the L1157 outflow, observed towards B1 by BP97. Figure 1 shows an example of our detect lines. We used the rotational diagram method to estimate the rotational temperature (T_{rot}) and column densities of the species for which we detect two or more transitions (see, e.g., Bisschop et al. 2007). We only detect one transition of $\text{C}_2\text{H}_5\text{OH}$, so we estimate its column density assuming $T_{rot} \sim 25 \text{ K}$ (similar to that of HCOOCH_3) and follow Requena-Torres et al. (2006). For all lines we assume the emission is optically thin and the gas is in local thermodynamic equilibrium. In Table 2 we show our results with a correction for beam dilution, assuming a source size of 10.5''. We base our assumption of the source size on the high-resolution interferometer CH_3OH observations of the L1157 blueshifted lobe by Benedettini et al. (2007) which show that B1 is mostly made of two subclumps. Taken together, the emission from these two subclumps extends about 10.5'' (estimated from the geometric mean of the minor and major axis of the emission, see Figure 2 of Benedettini et al. 2007). Whether the complex molecules are formed as a by product of methanol in the warm gas or are ejected from the grain mantle with the methanol (see below), we expect the emission from the observed complex molecules to be coincident with that of CH_3OH (see also, Liu et al. 2001). The CH_3CN emission is not corrected for source size as the beam size for all three transitions of this molecule is smaller than 10.5''.

Our estimates indicate that most of the detected molecules have T_{rot} between 10 and 30 K. This is lower than the estimated gas temperature of B1 ($T \sim 80 - 300 \text{ K}$, see below), as well as significantly lower than the temperature needed to evaporate off most of the species present in icy grain mantles (e.g., van Dishoeck & Blake 1998). Even so, similar low temperatures have also been derived for the same complex molecules in the gas immediately surrounding low-mass protostars (Cazaux et al. 2003; Bottinelli et al. 2004; 2007). It is possible that the low estimates of T_{rot} are due to our poorly constrained rotational diagrams, as we only detect two to four transitions (mostly at low energies) for each molecule. In addition, non-LTE effects may influence the derived temperature from the rotational diagram (Goldsmith & Langer 1999). Shock-heated molecular gas takes only a few hundred years to

cool from 100 K to 20 K (Bergin et al. 1998), and it is plausible that some of the detected molecules come from gas that has cooled down to the estimated low temperatures. Further observations are needed to distinguish with certainty which of the scenarios suggested above affect our estimates.

We calculate the abundance of each molecule ($X = N/N_{H_2}$) using our estimate of the molecule’s column density (N) and the estimate of H_2 column density (N_{H_2}) towards B1 obtained by BP97. The latter was obtained from single-dish observations of high-velocity CO outflow emission and assuming a standard CO/ H_2 ratio of 10^{-4} . Uncertainties on the size of B1, the CO/ H_2 ratio and the opacity of the CO line introduce uncertainties on our estimate of the absolute value of the abundance. However, these uncertainties are less important when comparing the relative abundance between the different molecules.

3. Discussion

Our results clearly indicate that complex organic molecules can be found in outflows from low-mass stars. The interesting question that follows is, how are these complex molecules formed? The two main competing scenarios propose that complex organic molecules mainly form either in the warm gas phase or on grain surfaces. The gas phase models were originally conceived to explain the chemical richness of hot cores. In these objects the radiation from a massive protostar is believed to heat the dense ($n \sim 10^6 - 10^7 \text{ cm}^{-3}$) inner core to temperatures higher than 100 K where the icy grain mantles evaporate injecting molecules like H_2O , H_2CO , CH_3OH into the gas-phase (e.g., Kurtz et al. 2000). The gas phase models indicate that subsequent chemical ion-molecule reactions in the warm gas can result in the formation of other, more complex, molecules, such as $HCOOCH_3$ and C_2H_5OH (the so called daughter or “second generation” species) (Charnley et al. 1992; Caselli et al. 1993). Alternatively, in the grain surface model, the observed complex organic molecules are formed on the grain surface and are later released into the gas phase (with H_2CO and CH_3OH) when the grain mantles evaporate (e.g., Hasegawa et al. 1992; Hasegawa & Herbst 1993).

In both models, a heat source is necessary to evaporate the icy grain mantle. At the position of B1, the outflow shock is the only source that can trigger the ejection of molecules from the grain surface. Using the known characteristics of the L1157 outflow shocks, we can deduce which of the two mechanisms is most likely responsible for the formation of the detected complex molecules. Multi-transition millimeter observations of NH_3 , CO and SiO indicate that the gas associated with B1 has a temperature between 80 and 300 K and a density of about $3 \times 10^5 \text{ cm}^{-3}$ (Tafalla & Bachiller 1995; Umemoto et al. 1999; Hirano & Taniguchi 2001; Nisini et al. 2007). The shocked region associated with B1 extends no more

than $20''$ along the outflow axis (see H_2 image in Zhang et al. 2000), and Nisini et al. (2007) indicate that shocks in L1157 have velocities larger than $\sim 30 \text{ km s}^{-1}$. We, therefore, estimate the time it took the shock to transverse the area associated with B1 to be no more than about 1400 yrs. Molecular gas heated by a shock with a velocity of about 30 km s^{-1} takes a few hundred years to cool down below 100 K (Bergin et al. 1998). Hence, the gas in the B1 region has been above 100 K for no more than 2000 yrs.

The B1 region is hot enough for grain mantles to evaporate and it is dense enough for gas-phase chemical reactions that result in complex molecules to occur (e.g., Millar et al. 1991). However, gas-phase models predict the maximum abundance of complex molecules in the gas to occur between a few 10^4 yrs and a few 10^5 yrs after the parent molecules are released into the gas phase (see Millar et al. 1991) —considerably longer than the timescale estimated above— and the maximum abundance of HCOOCH_3 predicted by these models is a factor of ten less than our observed abundance. Moreover, recent results by Horn et al. (2004) indicate that gas-phase production of HCOOCH_3 is much less efficient than previously considered by gas-phase models. It is highly improbable that most of the observed complex molecules in the L1157 outflow are produced in the gas phase. We therefore conclude that the relatively high abundance of complex molecules in the L1157 outflow is better explained by the formation of these species on the grain surface and their subsequent release into the gas phase caused by the outflow shock. We note that our results do not discard the possibility of small differences in the formation mechanism of these molecules, and that a small fraction of some of the species may exist in the gas phase independent of outflow shocks. For example, HCOOH has been observed in a quiescent dark cloud, yet HCOOCH_3 has only been observed in active regions (Turner et al. 1999; Requena-Torres et al. 2007). The derived HCOOH abundance in these studies is about 10^{-10} , two orders of magnitude smaller than our abundance estimates in L1157. Hence, only a negligible fraction of the complex species observed in L1157 could be due to processes unrelated to the outflow shock.

Recent surveys of abundances of complex species in hot cores, hot corinos, (the presumed low-mass counterparts of hot cores), and molecular clouds in the galactic center (GC) region favor the grain surface formation scenario (e.g., Bottinelli et al. 2007; Bisschop et al. 2007; Requena-Torres et al. 2006; 2007). The abundance ratio of the complex molecules with respect to CH_3OH (another, more abundant, grain mantle constituent) can be used to investigate the origin and evolution of these complex species (e.g., Bottinelli et al. 2007). Using the abundance of CH_3OH in B1 reported by BP97 (about 10^{-5}), we derive the abundance ratios $\text{HCOOCH}_3/\text{CH}_3\text{OH}$, $\text{HCOOH}/\text{CH}_3\text{OH}$, $\text{C}_2\text{H}_5\text{OH}/\text{CH}_3\text{OH}$, and $\text{CH}_3\text{CN}/\text{CH}_3\text{OH}$ to be in the order of 10^{-2} , 10^{-3} , 10^{-3} , and 10^{-5} respectively. The first three are in agreement (within an order of magnitude) with the average abundance ratios found in hot cores and molecular clouds in the GC region (Requena-Torres et al. 2006; Bisschop et al. 2007), and are

also consistent with the upper limits obtained toward the L1448 outflow by Requena-Torres et al. (2007). Taken together these results suggest the dust in hot cores, GC molecular clouds, and the L1157 molecular cloud have similar mantle composition (as also argued by Requena-Torres et al. 2006; 2007). In hot corinos, unlike the other sources, the abundance of HCOOCH_3 and HCOOH with respect to methanol is two orders of magnitude higher than in the B1 position of L1157. Such high relative abundance in hot corinos could be due to a longer warm-up phase of the gas surrounding low-mass protostars, when complex species are produced relatively more efficiently (Garrod & Herbst 2006). The CH_3CN to CH_3OH ratio is significantly lower by about three orders of magnitude for B1 than for hot cores and hot corinos (it has not been measured for GC clouds). One possible explanation for the low $\text{CH}_3\text{CN}/\text{CH}_3\text{OH}$ in B1 could be that processes in the shocked region (but not present in hot cores or hot corinos) rapidly destroy CH_3CN once it is in the gas phase. It is also possible that CH_3CN is truly a daughter specie and it shows very low abundance because there has not been enough time ($< 2 \times 10^3$ yr) for large abundances of this molecule to form in the warm gas associated with B1. With our current data we cannot confidently state which scenario is more likely and further observations are needed.

Similar abundance ratios of a number of molecules in the L1157 outflow (and in hot cores) compared to the abundance ratio of molecules in the comet Hale-Bopp led Bockelée-Morvan et al. (2000) to argue that there is a direct link between cometary and interstellar ices. The estimates of $\text{HCOOCH}_3/\text{CH}_3\text{OH}$ and $\text{HCOOH}/\text{CH}_3\text{OH}$ we obtain for L1157 are roughly similar to those of Hale-Bopp. Our results are consistent with the conclusions reached by Bockelée-Morvan et al. (2000) that molecules in cometary ices could have formed by processes very similar to those that produce the chemically rich icy mantles on interstellar grains.

In summary, our results clearly indicate that in molecular clouds with only low-mass star formation complex organic molecules can form through grain surface reactions. Outflow shocks can heat the surrounding medium and evaporate the icy grain mantles where the complex species reside, thereby releasing them into the gas phase and chemically enriching the circumstellar environment. Our results show that a protostar’s radiation is not the sole mechanism that can generate complex molecules near forming stars and that the impact of outflows needs to be considered when studying complex species around protostars. If no subsequent chemical reactions alter the abundance of complex molecules once they are released into the gas phase by the shock, then the abundance estimates from millimeter observations can be used to study the mantle composition of the dust in the cloud. Comparing the results from our observations of the B1 clump in the L1157 outflow with those of other regions observed by others suggest that the grain mantle composition in the L1157 dark cloud is comparable to that of the grains in hot cores and molecular clouds in the Galactic

center region. Observations of more complex molecules and estimates of their relative abundance towards other chemically active outflows will allow us to determine the reliability of millimeter observations of shocked molecular gas for estimating the abundance of complex molecules in grains and if similar grain mantle compositions are found in different regions of low-mass star formation.

REFERENCES

- Arce, H. G., & Sargent, A. I. 2006, *ApJ*, 646, 1070
- Bachiller, R., & Pérez Gutiérrez, M. 1997, *ApJ*, 487, L93 (BP97)
- Bachiller, R., Pérez Gutiérrez, M., Kumar, M. S. N., Tafalla, M. 2001, *A&A*, 372, 899
- Bergin, E. A., Melnick, G. J., Neufeld, D. A. 1998, *ApJ*, 499, 777
- Benedettini, M., et al. 2007, *MNRAS*, 381, 1127
- Bisschop, S. E., et al. 2007, *A&A*, 465, 913
- Bockelée-Morvan, D., et al. 2000, *A&A*, 353, 1101
- Bottinelli, S., et al. 2004, *ApJ*, 615, 354
- Bottinelli, S., Ceccarelli, C., Williams, J. P., & Lefloch, B. 2007, *A&A*, 463, 601
- Cabrit, S., et al. 1998, in *ASP Conf. Ser. 132, Star Formation with the Infrared Space Observatory*, ed. J. Yun & L. Liseau (San Francisco: ASP), 326
- Casselli, P., Hasegawa, T. I., & Herbst, E. 1993, *ApJ*, 408, 548
- Chandler, C. J., Brogan, C. L., Shirley, Y. L., & Loinard, L. 2005, *ApJ*, 632, 371
- Charnley, S. B., Tielens, A. G. G. M., & Rodgers, S. D. 1997, *ApJ*, 482, L203
- Cazaux, S., et al. 2003, *ApJ*, 593, L51
- Davis, C. J., & Eislöeffel, J. 1995, *A&A*, 300, 851
- Garay, G., et al. 1998, *ApJ*, 509, 768
- Garrod, R. T., & Herbst, E. 2006, *A&A*, 457, 927
- Goldsmith, P. F., Langer, W. D. 1999, *ApJ*, 517, 209

- Gueth, F., Guilloteau, S., & Bachiller, R. 1996, *A&A*, 307, 891
- Hasegawa, T. I., & Herbst, E. 1993, *MNRAS*, 263, 589
- Hasegawa, T. I., Herbst, E., & Leung, C. M. 1992, *ApJS*, 82, 167
- Hirano, N., & Taniguchi, Y. 2001, *ApJ*, 550, L219
- Horn, A., et al. 2004, *ApJ*, 611, 605
- Jørgensen, J. K., et al. 2007, *ApJ*, 659, 479
- Kurtz, S., et al. 2000, in *Protostars & Planets IV*, ed. V. Mannings, A. Boss & S. Russell (Tucson: Univ. Arizona Press), 299
- Liu, S.-Y., Mehringer, D. M., Snyder, L. E., 2001 *ApJ*, 552, 654
- Looney, L. W., Tobin, J. J., & Kwon, W. 2007, *ApJ*, 670, L131
- Millar, T. J., Herbst, E., & Charnley, S. B. 1991, *ApJ*, 369, 147
- Müller, H. S. P., Thorwirth, S. , Roth, D. A., & Winnewisser, G. 2001, *A&A*, 370, L49
- Nisini, B., et al. 2007, *A&A*, 462, 163
- Pickett, H. M., Poynter, R. L., Cohen, E. A., Delitsky, M. L., Pearson, J. C., & Müller, H. S. P. 1998, *J. Quant. Spectrosc. & Rad. Transfer* 60, 883
- Remijan, A. J., & Hollis, J. M. 2006, *ApJ*, 640, 842
- Requena-Torres, M. A., et al. 2007, *ApJ*, 655, L37
- Requena-Torres, M. A., et al. 2006, *A&A*, 455, 971
- Rohlfs, K., & Wilson, T. L. 2000, *Tools of Radio Astronomy* (3rd ed.; New York: Springer)
- Tafalla, M., & Bachiller, R. 1995, 443, L37
- Turner, B. E., Terzieva, R., & Herbst, E. 1999, *ApJ*, 518, 699
- Umemoto, T., et al. 1992, *ApJ*, 392, L83
- van Dishoeck, E. F., & Blake, G. A. 1998, *ARA&A*, 36, 317
- Zhang, Q., Ho, P. T. P., Wright, M. C. H., & Wilner, D. J. 1995, *ApJ*, 451, 71

Table 1. Detected Emission Lines

Molecule	Transition Line	Frequency [MHz]	E_u/k [K]	δv^a [km s ⁻¹]	T_{mb}^b [mK]	ΔV^c [km s ⁻¹]	$\int T_{mb} dV^d$ [K km s ⁻¹]	rms [mK]
HCOOCH ₃ -A	7 _{2,5} – 6 _{2,4}	90156.48	19.68	2.1	11	5.0 ± 1.5	0.06 ± 0.02	2
	8 _{0,8} – 7 _{0,7}	90229.63	20.07	1.0	12	3.7 ± 1.5	0.05 ± 0.02	3
	8 _{3,6} – 7 _{3,5}	98611.15	27.26	1.0	15	4.5 ± 0.9	0.07 ± 0.02	3
	8 _{4,5} – 7 _{4,4}	98682.60	31.90	3.0	7	3.3 ± 2.5	0.03 ± 0.03	2
	20 _{2,19} – 19 _{2,18}	226718.70	120.27	0.8	26	2.3 ± 0.8	0.07 ± 0.03	8
HCOOCH ₃ -E	7 _{2,5} – 6 _{2,4}	90145.72	19.69	1.0	12	5.7 ± 1.0	0.07 ± 0.02	2
	8 _{0,8} – 7 _{0,7}	90227.63	20.10	1.0	12	3.0 ± 0.7	0.04 ± 0.01	3
	8 _{3,6} – 7 _{3,5}	98606.85	27.28	1.0	11	3.3 ± 1.2	0.04 ± 0.02	3
	8 _{4,5} – 7 _{4,4}	98712.06	31.91	3.0	7	5.5 ± 2.3	0.04 ± 0.02	2
CH ₃ CN	14 ₃ – 13 ₃	257482.80	156.77	1.2	26	4.7 ± 1.2	0.13 ± 0.04	7
	14 ₁ – 13 ₁	257522.50	99.89	1.2	23	4.0 ± 1.0	0.10 ± 0.03	7
	14 ₀ – 13 ₀	257527.40	92.78	1.5	34	3.6 ± 1.0	0.14 ± 0.04	6
HCOOH	4 _{2,2} – 3 _{2,1}	90164.63	23.54	3.3	8	7.3 ± 1.8	0.06 ± 0.02	2
	6 _{2,4} – 5 _{2,3}	135737.76	35.48	1.4	17	5.8 ± 1.4	0.11 ± 0.03	3
C ₂ H ₅ OH	4 _{1,4} – 3 _{0,3}	90117.61	9.36	3.3	10	6.9 ± 1.0	0.08 ± 0.02	2

^aWidth of velocity channel.

^bPeak intensity from Gaussian fit to line.

^cVelocity width and error from Gaussian fit to emission line.

^dErrors in the integrated intensity estimate come from propagation of errors, using the error in the velocity width and the rms.

Table 2. Estimates of Temperature, Column Density and Abundance

Molecule	T_{rot} [K]	N [10^{13} cm^{-2}]	$X = N/N_{H_2}$ [10^{-8}]
HCOOCH ₃ -A ^a	27 ± 4	15 ± 4	11 ± 3
HCOOCH ₃ -E ^a	18 ± 13	12 ± 11	8 ± 7
CH ₃ CN ^a	110 ± 50	0.1 ± 0.05	0.07 ± 0.04
HCOOH ^b	10	8	5
C ₂ H ₅ OH ^c	25 ^d	10	7

^aError estimates come from linear fit to rotational diagram.

^bNo error estimate included as only two points were used for linear fit to rotational diagram.

^cNo error estimate included as column density was not obtained using the rotational diagram, see text.

^d T_{rot} assumed to be similar to the one derived for HCOOCH₃.

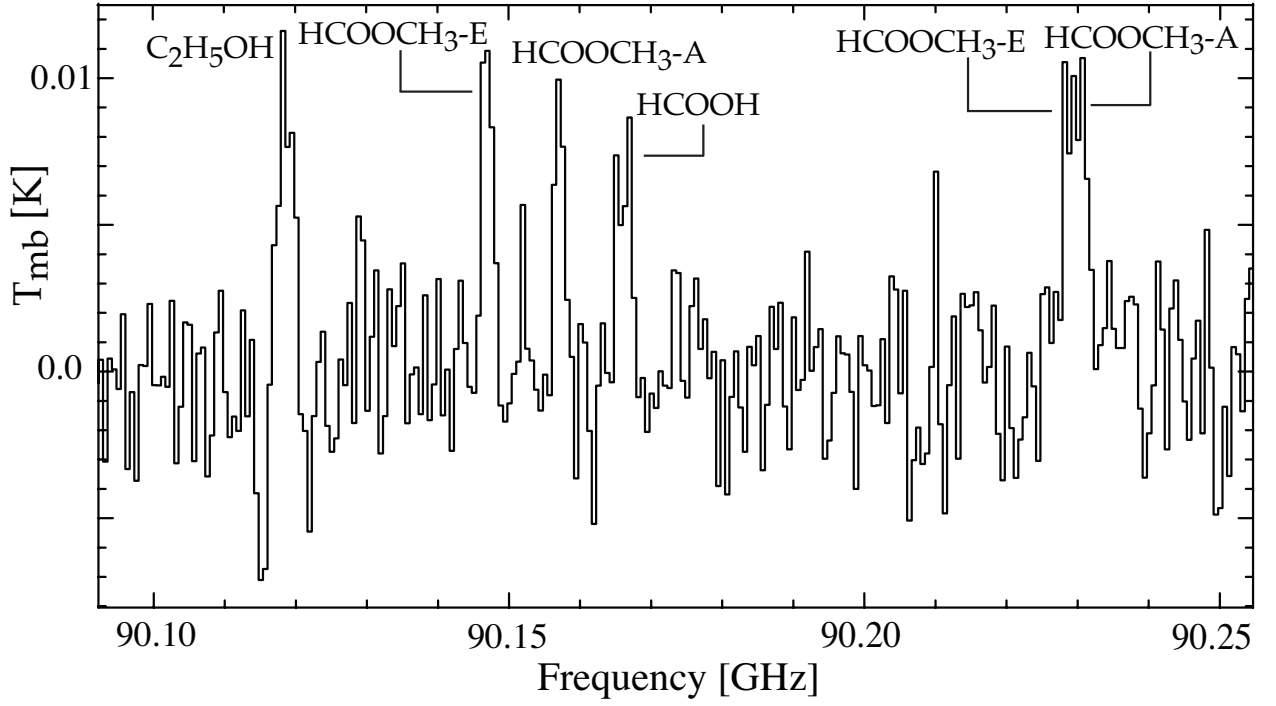


Fig. 1.— Sample spectrum from our observations of the B1 position in the L1157 outflow. The spectrum shown here is centered around 90.17 GHz, spans about 0.15 GHz, has a spectral resolution of 0.625 MHz ($\sim 2 \text{ km s}^{-1}$) and an rms of 2 mK.

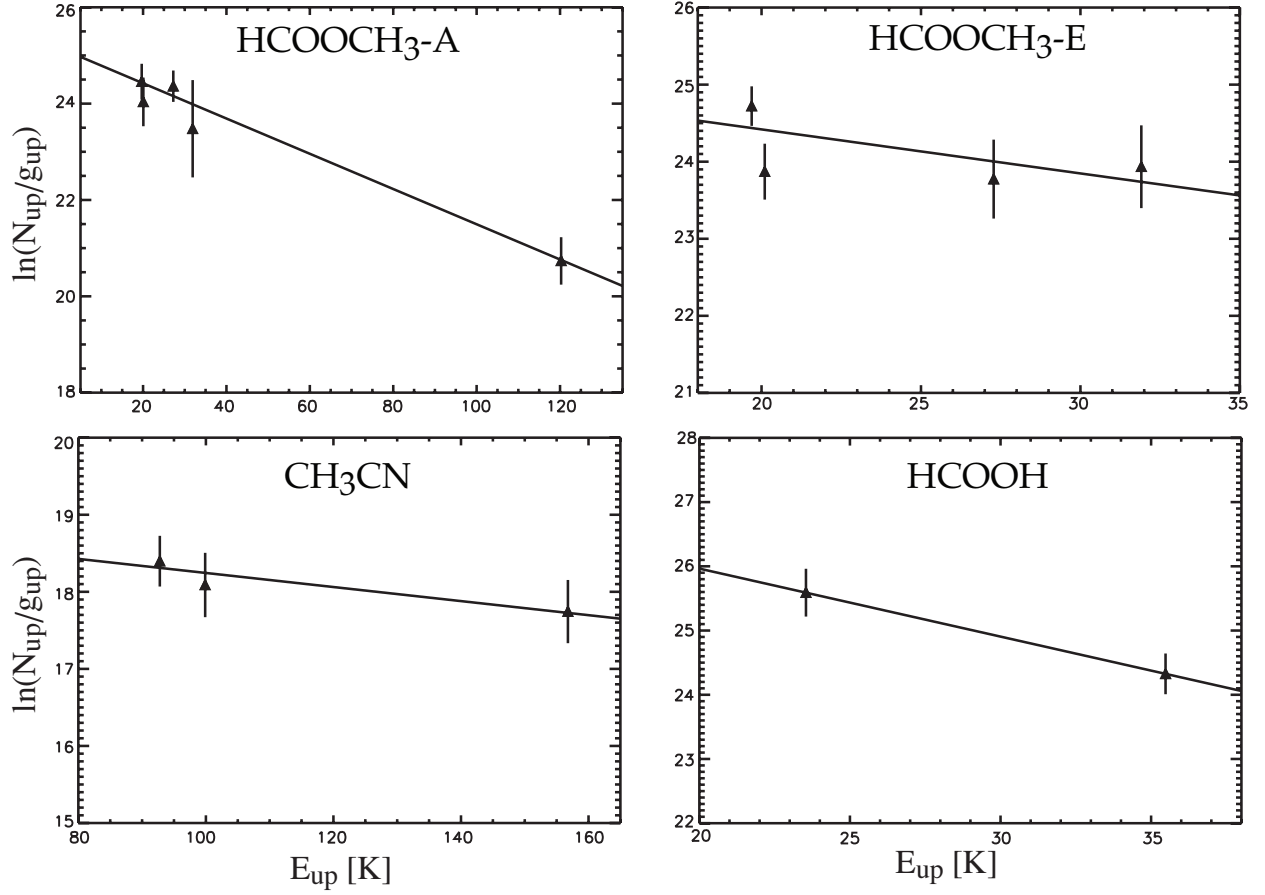


Fig. 2.— Rotational diagrams of molecules for which we detect two or more transitional lines. Errors shown are derived from the errors in the integrated intensity (see Table 1).